DIRAC NOTE 2001-01

Parameterisation of correlated and accidental particle spectra

Armando Lanaro (CERN)

March 14, 2001

Abstract

The Q distribution of accidental pairs is used in the DIRAC analysis to construct a function which describes the Q dependence of free (time-correlated) pairs through a well known fitting procedure applied in the range Q>4 MeV/c. This procedure yields correct results if, at rather large values of Q (Q>100 MeV/c), the ratio of experimental Q distributions from free pairs, dominantly non-Coulomb pairs from long-lived sources, to accidental pairs is flat. Therefore, the underlying assumption is that the inclusive production of correlated and accidental pion pairs have rather similar features.

Hereafter, we will test such assumption.

1 Introduction

At DIRAC center-of-mass energy ($\sqrt{s}$=6.84 GeV) time correlated pion pairs, produced inclusively in one-single proton-nucleon interaction, have a rather softer momentum spectrum than accidental pairs, produced in two successive proton interactions. This is because the latter have a larger available phase-space than the former. It can be seen from the slope of the momentum dependence of the ratio of correlated to accidental events (Fig. 1).

The assumption that the Q distribution of accidental pairs properly describes the Q distribution of free non-Coulomb pairs, and, thereafter, allows to construct a suitable function to describe the entire population of free (Coulomb plus non-Coulomb) pairs, relies on the fact that the above ratio is flat, at least over the range of momenta characteristics of pions from atomic pairs entering the DIRAC apparatus (p<4 GeV/c). Since this is not the case, as shown in Fig. 1, the subtraction procedure which yields the number of atomic pairs for, say, Q<3 MeV/c, might lead to an inaccurate result, to some extent.

It is the purpose of this report to illustrate a corrective procedure which validates the above assumption.

The starting point of this study is to consider inclusive charged pion spectra from both correlated and accidental events, and to parameterise such distributions using an universal

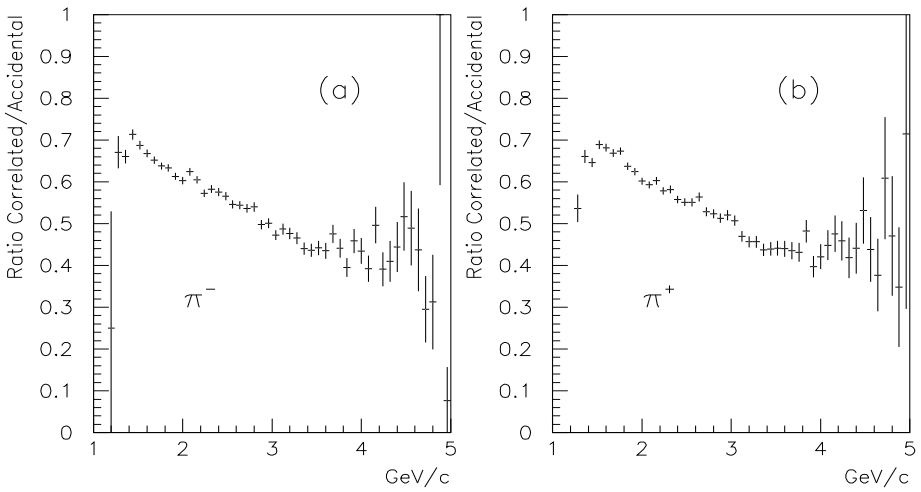

Figure 1: Ratio of momentum distributions of: a) correlated to accidental π^-, and b) correlated to accidental π^+. Events come from a sample of 2000 data collected with the Ni target and a cut on Q_L of the pair ($|Q_L|$ >20 MeV/c) has been applied.

function of the transverse momentum, p_T, and the Feynman-x (x_F) variables. The form of such function has been proposed [1] to describe the inclusive production of charged pions and kaons from proton-proton and proton-nucleus interactions in a wide range of incoming proton energies (from 6.6 GeV to 300 GeV).

Furthermore, a similar function is used to parameterise the distribution of the ratio of correlated to accidental events (of the type shown in Fig. 1). Such function is used to define an event weight applied only to accidental pions to yield a flat ratio of the distribution of correlated to accidental events.

Finally, the effect that such weighting procedure has on the calculated number of atomic pairs is evaluated in order to establish the degree of sensitivity.

2 Inclusive pion spectra from an unbiased data sample

For the study of inclusive pion spectra, from both accidental and correlated events, a sample of "minimum bias" data was collected during the 2000 experimental run using a Ni target (RUN 2917). Data were recorded using T1 as the main trigger without the coplanarity criterion and excluding the IH from the decision. The data sample was then processed using Ariane version 204.

The momentum spectrum of accidental π^- is shown in Fig. 2a before (histogram) and

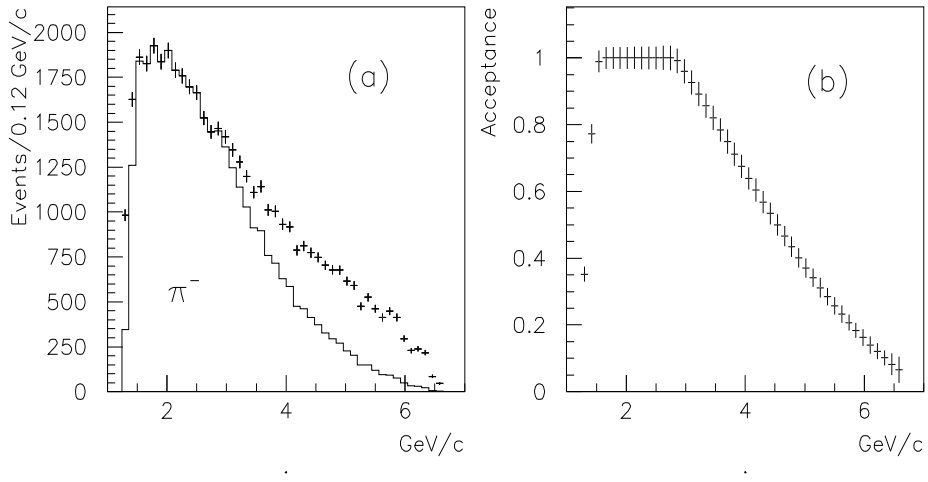

Figure 2: Experimental momentum distributions of accidental π^- before (histogram) and after (crosses) the acceptance correction (a). The momentum acceptance of the apparatus is shown in (b).

after (crosses) the correction for the geometrical apparatus acceptance (Fig. 2b) is applied. Accidental pions were defined as the events which have a hit time difference between vertical hodoscope arms in the range -4< Δt <-11 ns and 7< Δt <11 ns.

2.1 Apparatus geometrical acceptance

The acceptance correction has been evaluated on the basis of the momentum dependence of the x-coordinate of the hit associated to the track, measured by the SFD detector.

This is shown in the bidimensional plots of Fig. 3, for both sign particles. We observe unitary acceptance only for momenta between 1.6 GeV/c and 3 GeV/c. Outside this range the acceptance weight, at a fixed value of the momentum, has been evaluated as the fraction of the SFD x-plane where track hits are present. This approach assumes a uniform population over the scatter plot, that is only a first order approximation, which gives the advantage to apply the acceptance correction on an event-by-event basis. A more accurate evaluation of the geometrical acceptance would be possible by performing a Monte Carlo generation of events in a two-dimensional grid, in p_T and x_F for example, (or p_T and y, where y is the rapidity variable), then propagating the events through the apparatus and evaluating the fraction of events entering the fiducial volume. In this case, however, data need to be binned in pre-defined intervals in order to properly apply the acceptance correction.

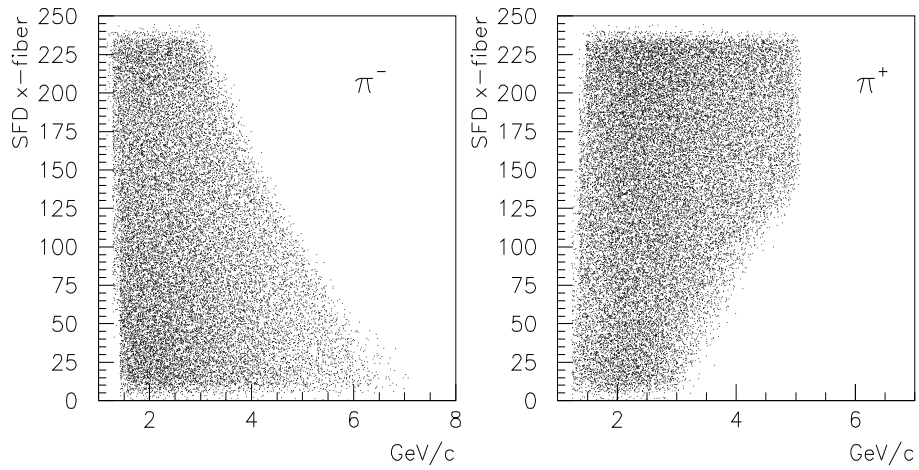

Figure 3: Hit SFD x-fiber column versus track momentum for π^- (left) and π^+ (right) particles. Events with $p(\pi^+)$ >5 GeV/c have been deliberately removed from the sample of correlated π^+ to decrease proton contamination.

2.2 Proton contamination

The sample of positive particles includes, besides π^+ (and some K^+, neglected hereafter), a large fraction of proton admixture, especially for large values of momentum. Proton contamination in the sample of correlated pairs is minimized by selecting events within a sufficiently narrow window in the distribution of the hit time difference between vertical hodoscope arms (-0.5< Δt <0.5 ns), and by applying a cut on the absolute value of the momentum of positive particle ($p(\pi^+)$ >5 GeV/c). Viceversa, the fraction of protons in the sample of positive particles from accidental events was evaluated at each momentum value and a weighting procedure was applied based on the momentum dependence of the ratio $\pi^+/(\pi^+ + p)$.

Single particle production rates have been measured and tabulated by Eichten and collaborators [2] in inclusive production of π, K, p and $\bar{p}$ by 24 GeV/c proton collisions on several nuclear targets (Be, Al, Cu, Pb). Particle rates were measured over a range of production angles from 17 to 127 mrad, and momenta from 4 to 18 GeV/c. To correct our Ni data we used tabulated rates measured at 107 mrad production angle, from proton-Cu collisions. For particle momenta below 4 GeV/c, were Eichten data are absent, we calculated the momentum dependence of the ratio $\pi^+/(\pi^+ + p)$ using the measured proportions of $\pi^-\pi^+$ and $\pi^- p$ pairs (from time-of-flight measurements) in a sample of correlated events (for details see A. Lopez-Aguera report). In order to be able to combine the two data sets (Eichten and DIRAC), DIRAC values were corrected at each momentum value for the decay probability of π^+ (and

K^+) along 11m flying-path. The momentum dependence of the fraction of π^+ is shown in Fig. 4b, and the compatibility of DIRAC low momentum with Eichten high momentum data appears satisfactory.

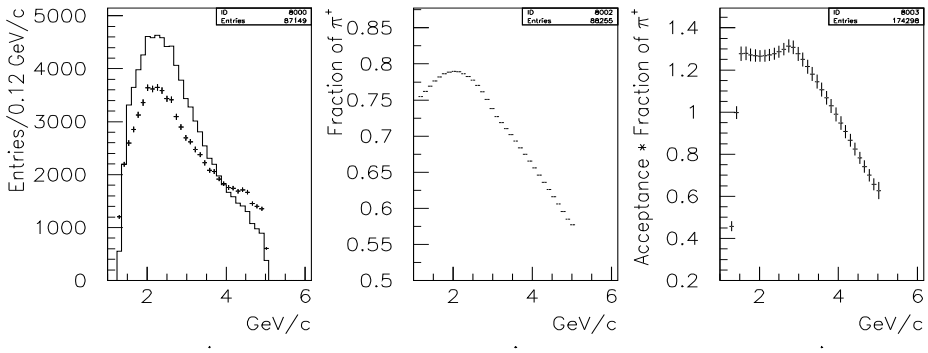

Figure 4: Experimental momentum distributions of accidental π^+ before (histogram) and after (crosses) correcting for the geometrical acceptance and proton contamination (a). (b) The momentum dependence of the ratio $(\pi^+ + K^+)/(\pi^+ + K^+ + p)$: DIRAC data for p$\leq$3.5 GeV/$c$, Eichten [2] data for p$\geq$4 GeV/$c$. The momentum dependence of the geometrical acceptance times the fraction of positive pions is shown in (c).

The momentum spectrum of accidental π^+ is shown in Fig. 4a before (histogram) and after (crosses) correcting for the geometrical acceptance of the apparatus and the proton contamination (Fig. 4c).

2.3 Parameterisation of inclusive pion spectra

In 1977 Badhwar and collaborators [1] have successfully provided an analytic representation of the proton-proton and proton-nucleus invariant cross sections for the inclusive production of $\pi^{\pm}$ and $K^{\pm}$. Available experimental data extended over the incident proton energy ranges from 6.6 to 1500 GeV, and from 12 to 300 GeV, for pp and pN collisions, respectively. The invariant cross section for production of pions of energy E, in the laboratory system, in proton-proton collisions is described by an analytic function of p_T and x_L^*:

$$E\frac{d^3\sigma}{d^3p} = \frac{A}{(1+\frac{4m_p^2}{s})^r}\,(1-\chi)^q\, exp\,[-Bp_T/(1+\frac{4m_p^2}{s})] = F(\chi, p_T) \qquad (1)$$

where χ is defined as:

$$\chi = \sqrt{x_L^{*2} + \frac{4}{s}(p_T^2 + m_\pi^2)} \qquad (2)$$

with x_L^* equal to the ratio of the parallel component of the center-of-mass momentum to the maximum transferable momentum and $\sqrt{s}$ is the total center-of-mass energy. The exponent q is a function of p_T and s such that:

$$q = (C_1 + C_2 p_T + C_3 p_T^2)/\sqrt{1 + 4m_p^2/s} \tag{3}$$

and A, B, C_1, C_2, C_3 and r are fitting parameters.

We have used a similar expression with the only exception of adopting the variable $x_F = 2p_z^*/\sqrt{s}$ instead of x_L^*. Simple algebra relates the pion momentum distribution dN/dp to the invariant cross section (1):

$$\frac{dN}{dp} = \frac{p^2 sin\theta}{E} F(\chi, p_T), \qquad sin\theta = p_T/p \tag{4}$$

and the use of jacobian transformations[1] allow to describe p_T and $(1-\chi)$ distributions in terms of the invariant cross section (1):

$$\frac{dN}{dp_T} \simeq 2p_T F(\chi, p_T), \qquad \frac{dN}{d(1-\chi)} \simeq \frac{p_T\sqrt{s}}{E^*} F(\chi, p_T) \tag{5}$$

A generalization of expression (1) to collisions of protons with nuclei is done [1] by taking into account:

- the probability that the incoming proton undergoes charge-exchange with the target neutron and behaves like a neutron;
- the interaction mean free path for pp and pN collisions.

Thus, for pN collisions, it follows that the invariant cross section per target nucleon for the production of $\pi^{\pm}$ can be parameterised as follows:

$$(E\frac{d^3\sigma}{d^3p})_{\pi^{\pm}} = \frac{\lambda_{pp}}{\lambda_{pN}}[\sigma_{\pm} + \eta f_n(\sigma_{\mp} - \sigma_{\pm}] \tag{6}$$

where σ_+ and σ_- are the invariant cross sections of π^+ and π^-, respectively, in pp collisions (1), f_n is the fraction of neutrons in the target nucleus, and λ_{pp} and λ_{pN} are the interaction mean free paths for pp and pN collisions, respectively[2]. The value of the "charge mixing parameter", η, has been set to the weighted average of a set of experimental values from collisions with light (Be) and heavy (Pb) nuclei, namely to 0.195 ($\pm$ 0.015). In order to fit our data, the values of the ratio $\lambda_{pp}/\lambda_{pN}$ were set to 47.6 and 81.2 for Ni and Pt nuclei, respectively.

2.4 $\pi^{\pm}$ from accidental events

In Fig. 5 the distributions of π^- from accidental events are shown as a function of p, p_T and $(1-\chi)$. Superimposed to the histograms is the analytic function (6), transformed according to the relations (4) and (5).

[1] $d^3p/E = \pi dy dp_T^2$, and $dy dp_T = \sqrt{s}/2E^* dx_F dp_T$, y is the rapidity variable= $1/2 ln[(E+p_z)/(E-p_z)]$.

[2] An error was detected in the analogous expression of ref.[1]

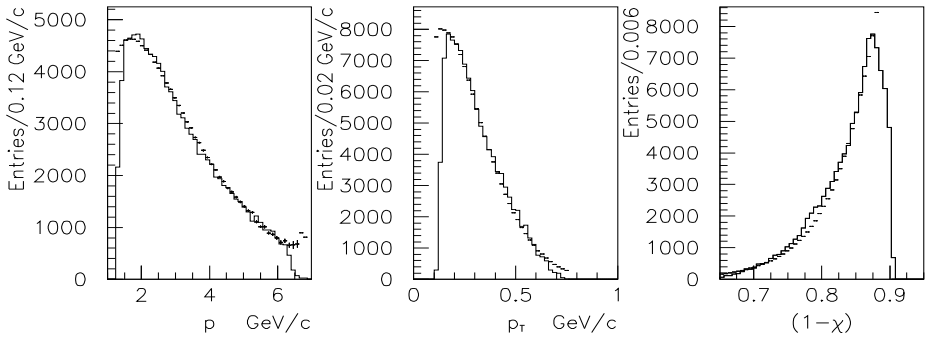

Figure 5: Experimental p, p_T and $(1-\chi)$ distributions of **accidental** π^- corrected for acceptance (histogram) with superimposed the results of the parameterisation (6).

Similarly, in Fig. 6, the experimental distributions and their parameterisation are shown for π^+ from accidental events.

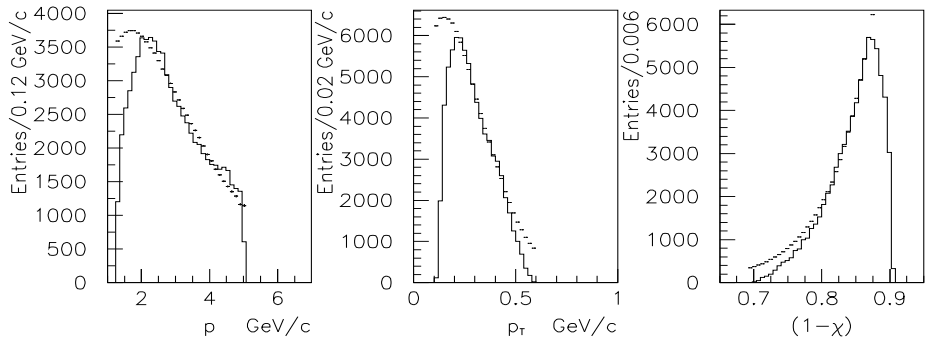

Figure 6: Experimental p, p_T and $(1-\chi)$ distributions of **accidental** π^+ corrected for acceptance and proton contamination (histogram) with superimposed the results of the parameterisation (6).

The general agreement is satisfactory and better in the case of π^- than for π^+ spectra. However, for the latter, one should take into account the influence of larger acceptance corrections, especially at higher values of p, p_T and χ, where stronger is the contamination from protons.

In Table 1 the values of the parameters of expression (1) are given. The parameter A of (1) is an unimportant normalization coefficient. We were able to describe DIRAC data using the

same parameter values as in the work of Badhwar [1] with the exception of the constant C_2.

Particle	B	r	C_1	C_2 $(\mathrm{GeV}/c)^{-1}$	C_3 $(\mathrm{GeV}/c)^{-2}$
π^-	5.3	3	7.0334	-2.5 (-4.5)	1.667
π^+	5.55	1	5.3667	-1.0 (-3.5)	0.8334

Table 1. Parameters for the representation of DIRAC experimental spectra of single particles from **accidental** events. The value of C_2 in parentheses is from ref.[1].

2.5 $\pi^{\pm}$ from correlated events

To describe the experimental distributions of pions from correlated events we have used a similar approach, namely we have considered single pions as if they were produced inclusively in one proton-nucleus collision and not in highly correlated pairs.

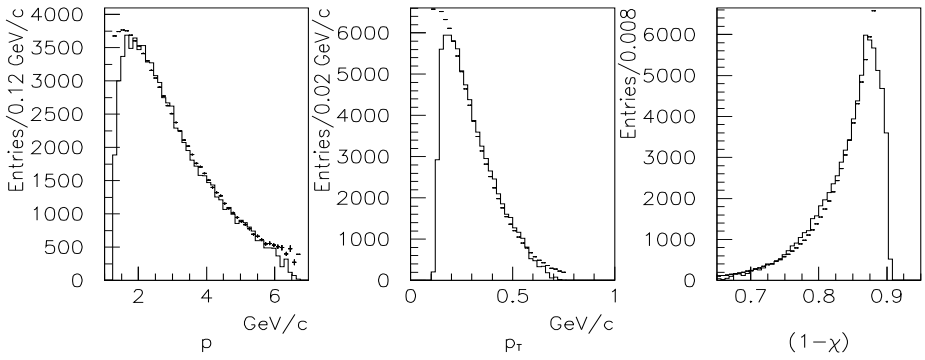

Figure 7: Experimental p, p_T and $(1-\chi)$ distributions of **correlated** π^- corrected for acceptance (histogram) with superimposed the results of the parameterisation (6).

Even with this approximation, however, we were able to describe the experimental single particle spectra in a quite satisfactory way. Fig. 7 and Fig. 8 show the experimental distributions and the parameterisation (1) superimposed to the data, for π^- and π^+, respectively. Both experimental spectra are corrected for the geometrical apparatus acceptance. Also, the proton admixture in the π^+ (and K^+) sample is considered negligible for correlated events, thus, no specific correction was applied in this case.

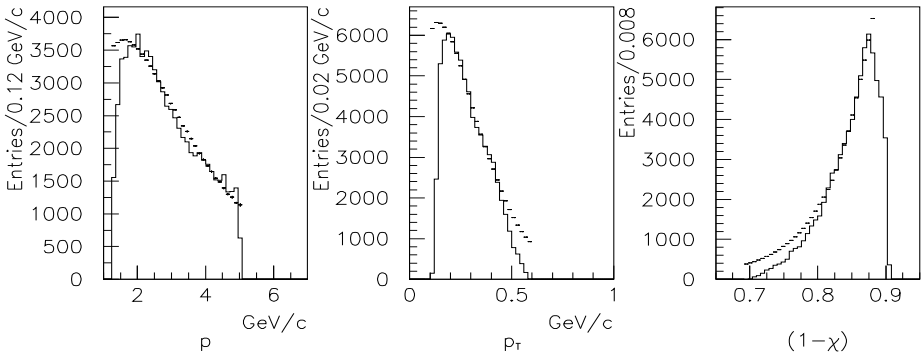

Figure 8: Experimental p, p_T and $(1-\chi)$ distributions of **correlated** π^+ corrected for acceptance (histogram) with superimposed the results of the parameterisation (6).

Particle	B	r	C_1	C_2 $(\mathrm{GeV}/c)^{-1}$	C_3 $(\mathrm{GeV}/c)^{-2}$
π^-	6.9	0.1	6.5	-3.5	1.667
π^+	6.35	0.1	4.5	-2.5	0.8334

Table 2. Parameters for the representation of DIRAC experimental spectra of single particles from **correlated** events.

Finally, in Table 2 the values of the parameters of expression (1) are given.

3 Ratio of real to accidental pions

The parameterisation of pions spectra from both accidental and correlated events allows to construct an analytic function of the type (6) for the ratio of real to accidental pions. The use of such analytic function as an event-by-event weight applied to the experimental spectra of pions from accidental events should modify the shape of spectra of the type shown in Fig. 1, and provide a flat distribution of the experimental ratio of real to accidental events as a function of any variable, like: p, p_T, $(1-\chi)$, Q, F.

The most obvious form for the analytic function would be:

$$(\frac{dN^{real}}{dN^{acc}})_{\pi^\pm} \simeq (1-\chi)^{\Delta q}\, exp\,[-\Delta B\, p_T/(1+\frac{4m_p^2}{s})] \qquad (7)$$

with $\Delta q = q^{real} - q^{acc}$ and $\Delta B = B^{real} - B^{acc}$.

A flat distribution of the ratio of real to accidental π^+ was obtained with little adjustment

of the values of ΔB, and, for both π^+ and π^-, an extra correction for the events in the low p_T region ($p_T \leq$0.21 GeV/c) was applied in addition[3].

Particle	ΔB	Δq	a	b $(\mathrm{GeV}/c)^{-1}$	c $(\mathrm{GeV}/c)^{-2}$
π^-	1.6	$q^{real} - q^{acc}$	0.42	3.8	10.
π^+	1.1	$q^{real} - q^{acc}$	1.6	-3.1	0.5

Table 3. Parameters for the representation of the experimental distribution of the ratio of real to accidental $\pi^{\pm}$.

The extra low-p_T correction was parameterised in terms of a second order polynomial ($a + bp_T + cp_T^2$). All parameter values are shown in Table 3, and Fig. 9 shows the distributions of the ratio of real to accidental for π^- (first row) and π^+ (second row), after applying the weighting procedure to accidental pions.

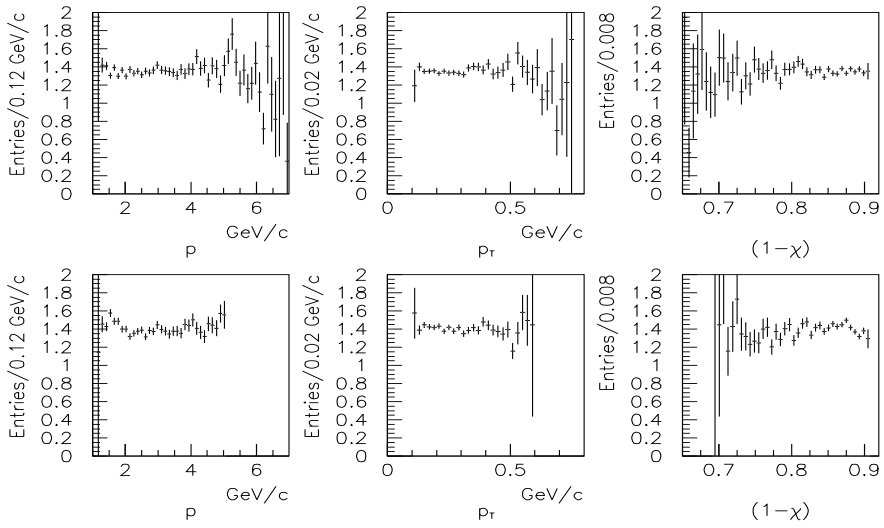

Figure 9: Experimental p, p_T and $(1-\chi)$ distributions of the ratio of real to accidental π^- (upper row) and π^+ (bottom row). Accidental events are weighted according to the parameterisation (7). Events come from a sample of unbiased data.

A straightforward application of the weighting procedure described above should allow, in principle, to obtain comparable shapes for the Q distributions of real and accidental events. In other words, one expects a flat Q dependence of the ratio of real to accidental events, and,

[3]we removed the dependence on the parameter r by a a slight readjustment of the ΔB parameter value

therefore, the possibility to describe the lineshape of one distribution (real) with the help of the other (accidental), as outlined in the introduction. The Q distribution of real and accidental events in shown in Fig. 10a, their ratio in Fig. 10b, for uncorrected accidental pairs. The Q range extends up to 250 MeV/c as data were recorded with the minimal trigger condition (T1). Fig. 10c shows the Q dependence of the ratio of real to accidental, after accidental events have been assigned a weight W given by:

$$W = (\frac{dN^{real}}{dN^{acc}})_{\pi^-} \times (\frac{dN^{real}}{dN^{acc}})_{\pi^+} \tag{8}$$

The corrected ratio shows now no dependence on Q. Nevertheless, a deviation from flatness is expected at very low values of Q (Q<50 MeV/c), where the Coulomb attraction should play its role.

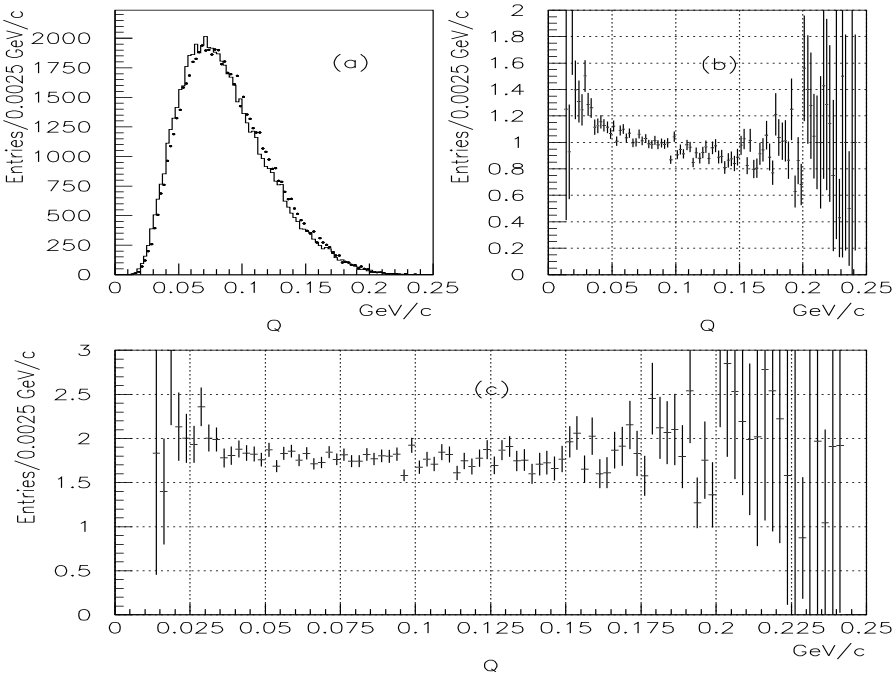

Figure 10: Experimental Q distributions for real (histogram) and accidental (points) pairs (a); Q dependence of the ratio of real to accidental events for (b) uncorrected and (c) corrected accidental pairs.

4 Extension to trigger-biased data samples

A generalization of the previous results to data samples collected with higher trigger levels (T2,T3,DNA,T4) is illustrated in the following.

4.1 Ratio of real to accidental pions

We begin our survey by considering a sample of events collected in 1999 with a Ni target using T2 as the main trigger. A selection on the absolute value of Q_L (Q_L >20 MeV/c) was applied to all data samples considered in this section in order to be less sensitive to the Coulomb attraction between correlated pions.

Fig. 11 shows the distributions of the ratio of real to accidental π^- before (upper row) and after (bottom row) the event-by-event weight (7) is applied to accidentals. Similar distributions, but for π^+ particles, are shown in Fig. 12. Table 4 summarizes the parameter values.

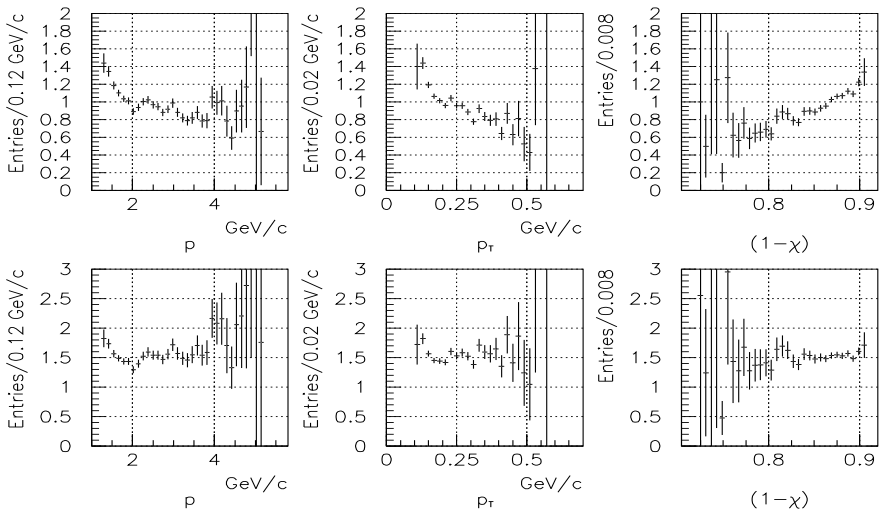

Figure 11: Experimental p, p_T and $(1-\chi)$ distributions of the ratio of real to accidental π^-, before (upper row) and after (bottom row) applying the weighting algorithm (7) to accidentals. Events come from a 1999 data sample collected with a Ni target and the T2 trigger.

Particle	ΔB	Δq	a	b $(\mathrm{GeV}/c)^{-1}$	c $(\mathrm{GeV}/c)^{-2}$
π^-	2.5	$q^{real} - q^{acc}$	-	-	-
π^+	1.6	$q^{real} - q^{acc}$	0.96	1.3	-7.4

Table 4. Parameters for the representation of the experimental distribution of the ratio of real to accidental $\pi^{\pm}$ for 1999 Ni data. No extra-correction was required for low p_T π^-.

We also applied our weighting procedure (7) to a sample of data collected in 1999 with a Pt target using the T3 trigger. Figs. 13 and 14 show the distributions of real to accidental π^- and π^+, respectively. The parameter values are the same used for correcting the nichel data (Table 3).

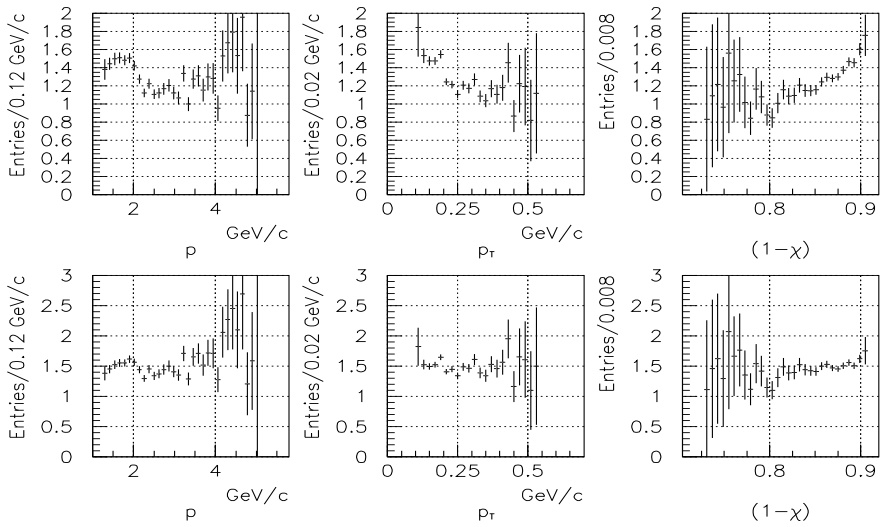

Figure 12: Experimental p, p_T and $(1-\chi)$ distributions of the ratio of real to accidental π^+, before (upper row) and after (bottom row) applying the weighting algorithm (7) to accidentals. Events come from a 1999 data sample collected with a Ni target and the T2 trigger.

Finally, similar distributions are shown in Figs. 15 and 16 for events coming from more recent data collected in 2000 with a Ni target and T3,DNA and T4 trigger definition. The parameter values were still those presented in Table 3.

4.2 Experimental Q distributions

The purpose of higher trigger levels is to select correlated and accidental pairs with very low-Q. This is shown in Fig. 17, and for comparison in Fig. 10a, where the Q spectra of real (17a) and accidental (17b) pairs are shown, for the different data samples considered above. Contrarily to the results obtained with the analysis of the unbiased data sample, here the application of the weighting algorithm produces no appreciable difference between the Q distributions of accidentals before and after the weight (8) is applied. As a consequence, the Q (and F) dependence of the ratio of real to accidental pairs is unchanged, and a distinct slope remains to characterize the distribution (Coulomb interaction in the final state), independently of the data sample used (Fig. 18). At larger values of Q, accessible with the unbiased event sample, no evidence of a definite slope was observed (Fig. 10c).

Finally, the Q dependence of the weights W, defined by (8), is shown in Fig. 19 for the 3 data samples.

In order to determine quantitatively the sensitivity of the physics result to the weighting procedure described above, we have recalculated the number of atomic pairs from the 3 data

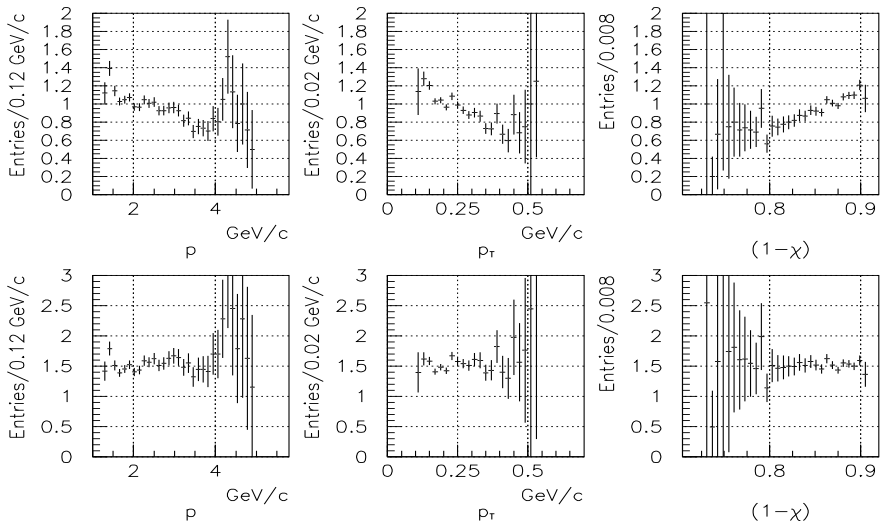

Figure 13: Experimental p, p_T and $(1-\chi)$ distributions of the ratio of real to accidental π^-, before (upper row) and after (bottom row) applying the weighting algorithm (7) to accidentals. Events come from a 1999 data sample collected with a Pt target and the T3 trigger. A cut on Q_L >20 MeV/c is applied.

samples (Ni and Pt 1999, Ni 2000) and compared it with the estimate based on unweighted accidental events. In the range F<3 the absolute difference between the two results, with and without weighting, is less than 0.2% for all data samples.

5 Conclusion

Inclusive spectra of pions from both accidental and correlated events, produced in DIRAC from 24 GeV/c proton-nucleus collisions, were successfully described using an analytic function of p_T and x_F.

A similar function was used to parameterise the ratio of real to accidental events. This parameterisation allows to correct the distribution of accidental events to yield a flat dependence of the ratio of real to accidental events on several kinematic variables (p, p_T and $(1-\chi)$), and for several data samples, both trigger biased and unbiased.

The weighting procedure produces a distribution of the ratio of real to corrected accidental pairs also flat in Q, at least for large values of Q (Q>40 MeV/c) (minimum bias data sample). For standard triggered events the weighting procedure produces no significative modification of the Q distribution of accidental events. As a consequence, the Q dependence of the ratio of real to corrected accidentals exhibits a definite slope at small values of Q (Q<30 MeV/c), due

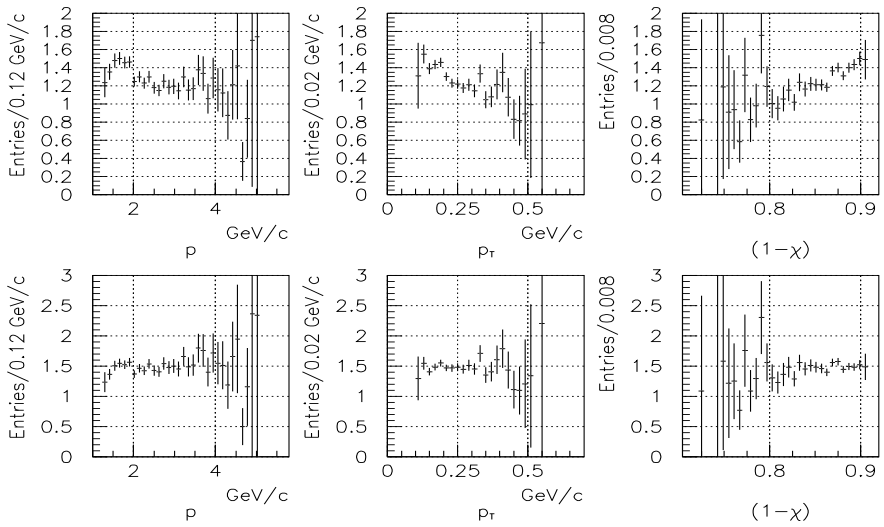

Figure 14: Experimental p, p_T and $(1-\chi)$ distributions of the ratio of real to accidental π^+, before (upper row) and after (bottom row) applying the weighting algorithm (7) to accidentals. Events come from a 1999 data sample collected with a Pt target and the T3 trigger. A cut on Q_L >20 MeV/c is applied.

to the influence of the Coulomb attraction between correlated pairs.

The sensitivity of the final result, i.e. the calculated number of atomic pairs, to the procedure described above is at the level of 0.2%.

References

[1] G.D. Badhwar, S.A. Stephens, R.L. Golden, *Phys. Rev.* D **15**, 820 (1977).

[2] T. Eichten et al., *Nucl. Phys.* B **44**, 333 (1972).

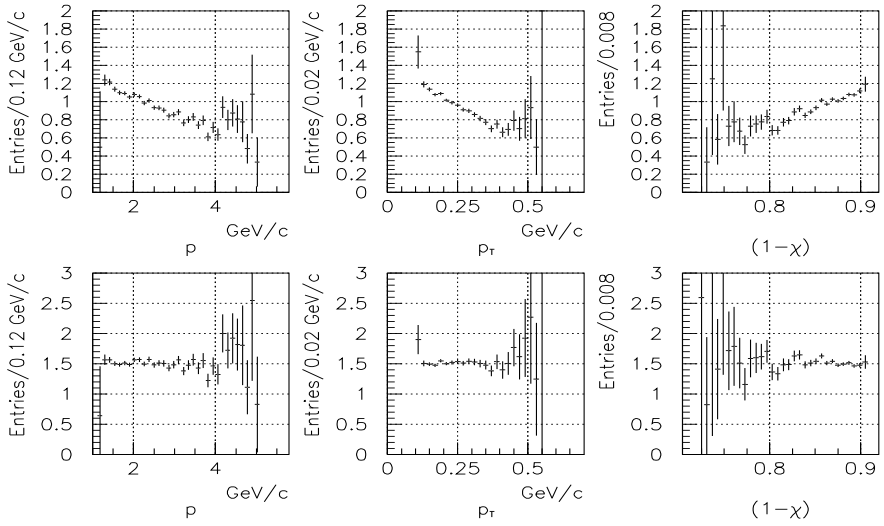

Figure 15: Experimental p, p_T and $(1-\chi)$ distributions of the ratio of real to accidental π^-, before (upper row) and after (bottom row) applying the weighting algorithm (7) to accidentals. Events come from a 2000 data sample collected with a Ni target and the T3, DNA and T4 trigger. A cut on Q_L >20 MeV/c is applied.

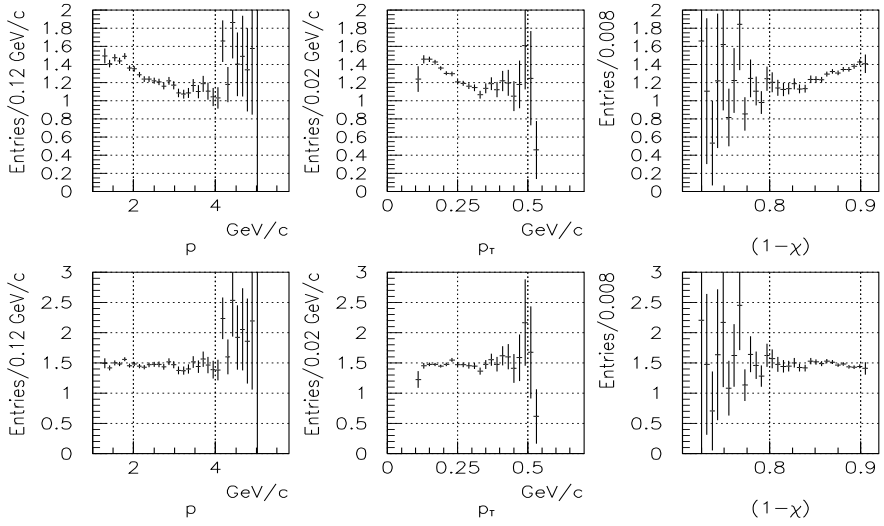

Figure 16: Experimental p, p_T and $(1-\chi)$ distributions of the ratio of real to accidental π^+, before (upper row) and after (bottom row) applying the weighting algorithm (7) to accidentals. Events come from a 2000 data sample collected with a Ni target and the T3, DNA and T4 trigger. A cut on Q_L >20 MeV/c is applied.

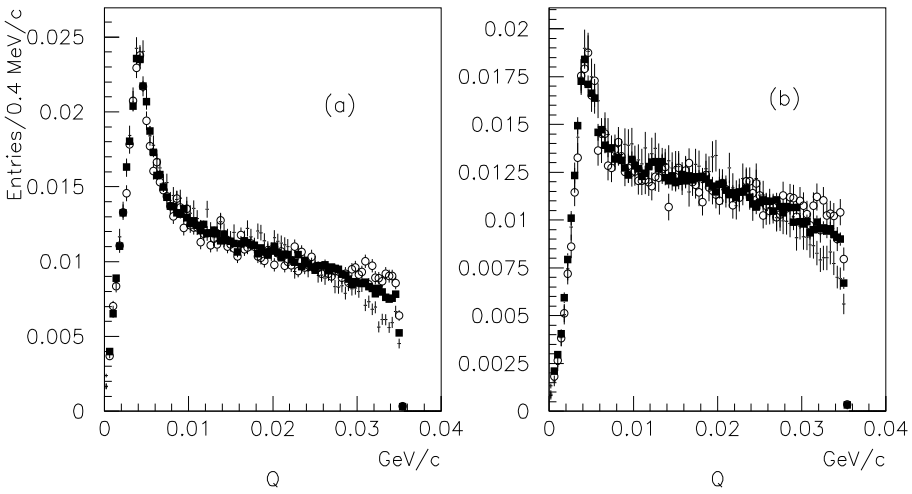

Figure 17: Normalized experimental Q distributions for (a) real and (b) accidental pairs from: 1999 Ni data (empty circles), 1999 Pt data (crosses) and 2000 Ni data (full squares).

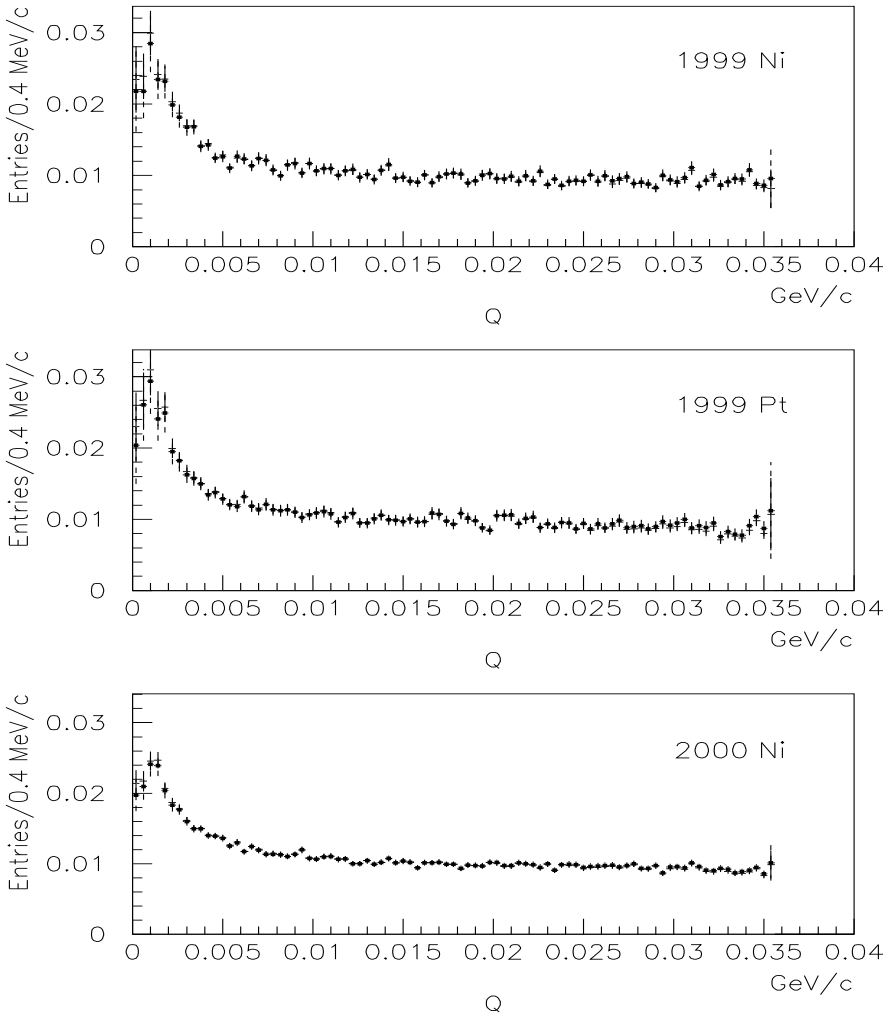

Figure 18: Q dependence of the ratio of real to accidental pairs before (crosses) and after (full squares) correcting the accidental events. Corrected and uncorrected distributions are almost indistinguishable.

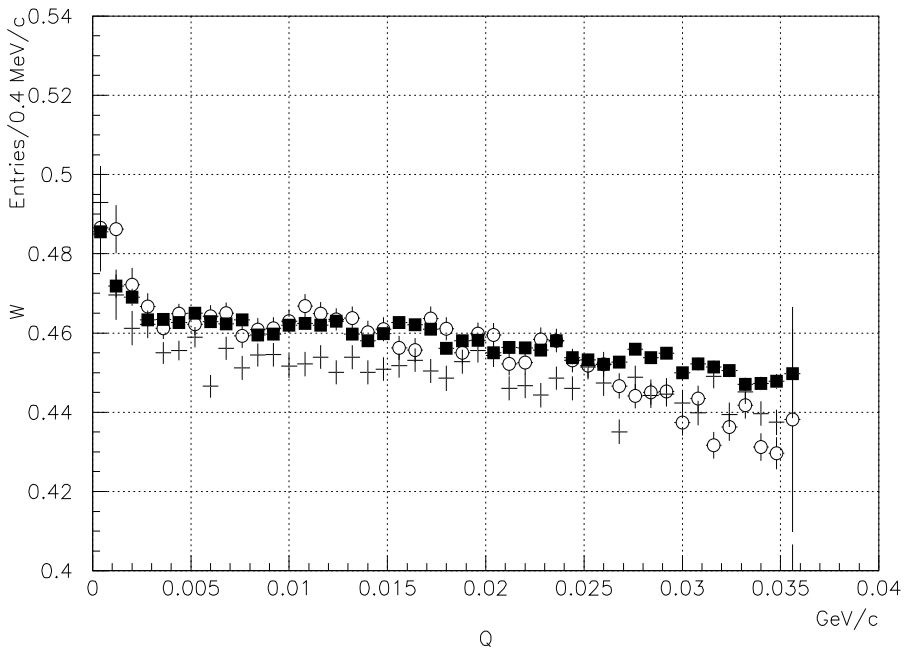

Figure 19: Q dependence of the weight W, defined by (8), for 1999 Ni data (crosses), 1999 Pt data (empty circles) and 2000 Ni data (full squares).